

NANO EXPRESS

Open Access



Synthesis of Fe and N Co-doped $\text{Bi}_2\text{Ti}_2\text{O}_7$ Nanofiber with Enhanced Photocatalytic Activity Under Visible Light Irradiation

Bitao Liu^{1*}, Qionghua Mo^{1,2}, Jiali Zhu¹, Zhupei Hou¹, Lingling Peng¹, Yijia Tu^{1,3*} and Qinyi Wang⁴**Abstract**

A series of N-Fe- $\text{Bi}_2\text{Ti}_2\text{O}_7$ nanofibers were successfully synthesized. The structure, morphology, visible light photocatalytic properties, and the degradation mechanism of N-Fe- $\text{Bi}_2\text{Ti}_2\text{O}_7$ were investigated. A new phase of $\text{Bi}_4\text{Ti}_3\text{O}_7$ and smaller band gap could be observed after doing Fe and N into $\text{Bi}_2\text{Ti}_2\text{O}_7$. It can degrade 66 % MO and 87 % MB in 120 min under visible light irradiation, which is much more than that of pure $\text{Bi}_2\text{Ti}_2\text{O}_7$. The results indicate that such unique structure could enhance the charge transfer between the nanostructure interfaces and therefore improve its photocatalytic activities.

Keywords: Photocatalysts, Semiconductors, Composite materials, Visible light

Background

In the past decades, industrial pollution introduced by the development of economy has caused lots of troubles. Photocatalyst is regarded as a promising potential solution to these environmental problems [1, 2]. TiO_2 semiconducting material has been extensively applied in the field of catalysis and considered as one of the best photocatalytic materials due to its strong oxidizing, long-term thermodynamic stability and relative nontoxicity [3]. However, due to its special band structure, the photogenerated electrons and holes in TiO_2 would undergo a rapid recombination, significantly decreasing the photocatalytic activity in the pollutants' degradation process [4]. More importantly, due to its large band gap, TiO_2 can utilize photons in the wavelength range less than 400 nm [5]. Therefore, the critical issue of improving the photocatalytic activity of TiO_2 is to effectively inhibit the recombination of photogenerated electron-hole pairs and extend the light absorption to the visible light region [6–8].

Recently, many Bi_2O_3 - TiO_2 (BTO)-based composites have been drawn much attention for their unique performance in photocatalysis [9–11]. $\text{Bi}_2\text{Ti}_2\text{O}_7$ was widely

studied due to its narrow band gap of 2.6 eV, which means it can absorb the visible light below 480 nm [12]. However, it still needs to improve the photocatalytic efficiency and enlarge the visible light absorbed range to realize indoor application of the photocatalyst [9–12].

In this work, the N- and Fe-doped $\text{Bi}_2\text{Ti}_2\text{O}_7$ nanofibers were prepared by a simple emulsion electrospinning process. After Fe and N doping, smaller band gap $\text{Bi}_2\text{Ti}_2\text{O}_7$ and newly $\text{Bi}_4\text{Ti}_3\text{O}_7$ phase can be observed. This would enlarge the light absorbed range and accelerate the separation of the electron-hole pairs; subsequently, the photocatalytic properties were investigated in detail.

Methods**Synthesis of BTO Fibers**

BTO fibers were prepared similar to the previous report [8]. As a typical progress, 4.26 g tetrabutyl titanate, 6 g DME, 0.8 g PVP ($M_w = 1300000$), 6.08 g $\text{Bi}(\text{NO}_3)_3 \cdot 5\text{H}_2\text{O}$, and $\text{FeCl}_3 \cdot 6\text{H}_2\text{O}$ were mixed and stirred for 12 h. The spinneret diameter was 0.9 mm, and the distance between the tip of the spinneret and the collector is 20 cm. A direct current voltage of 18 kV was maintained during the electrospun process. The as-prepared fibers were maintained at 600 °C for 2 h. Then, the samples were transfer into nitriding furnace maintained at 500 °C for 8 h.

* Correspondence: liubitao007@163.com; 275430858@qq.com

¹Research Institute for New Materials Technology, Chongqing University of Arts and Sciences, Yongchuan, Chongqing 402160, China
Full list of author information is available at the end of the article

Instruments

The instruments were similar to our previously work [13]. The X-ray diffraction (XRD) patterns were recorded by a Danton TD-3500 X-ray diffractometer (Cu-K α radiation, $\lambda = 1.54 \text{ \AA}$). Field emission scanning electron microscope (Hitachi, SU-8020) was used to acquire the scanning electron microscopy (SEM) images. Transmission electron microscopy (TEM) micrographs were taken with a JEOL-JEM-2010 (JEOL, Japan, 200 kV). X-ray photoelectron spectroscopy (XPS) analysis was performed on an ESCA Lab MKII X-ray photoelectron spectrometer (Mg K α). UV-vis absorption spectra of the samples were obtained on a UV-vis spectrophotometer (Hitachi, U-3900), and BaSO $_4$ powder was used as the substrate. The photoelectric performance was measured using an electrochemical system (CHI-660B, China). The counter and the reference electrodes were platinum wire and saturated Ag/AgCl, respectively. 0.1 M NaSO $_4$ solution was used as electrolyte solution for the measurement, a 150 W Xe arc lamp was utilized as the light source for the photoelectrochemical (PEC) measurement, and the photoresponse was measured at 0.0 V. Electrochemical impedance spectra (EIS) were recorded in the open circuit potential mode and the frequency was range from 100 kHz to 0.01 Hz.

Photocatalytic Activity Measurement

As reported in our previously work [13], the photocatalytic activities were evaluated under visible light irradiation using a Xe lamp light source with a 420-nm UV cutoff filter. In a typical process, 100 mg of photocatalyst was dispersed in 100-ml methylene blue (MB) and methyl orange (MO) aqueous solution (50 mg L $^{-1}$), respectively.

Before irradiation, the solution was stirred for 30 min in the dark to ensure the establishment of adsorption desorption equilibrium. Under light irradiation and stirring, 3-ml solution was taken at every 10 min, followed by centrifugation and filtration to remove the photocatalysts. The concentrations of dye were analyzed on a Varian UV-vis spectrophotometer (Cary-50, Varian Co.).

Results and Discussion

The morphology of the N-Fe-BTO 0.5 % samples were shown in Fig. 1. These nanofibers with the diameter of 100~150 nm were consisting with many nanoparticles, as shown in Fig. 1a, b. Obviously, this structure could result in high specific surface area and provide many active sites in the photocatalytic process [8]. And from the TEM images in Fig. 1c, d, clear lattice fringes were observed, indicating that these nanofibers have good crystallinity. The interplanar distances was 0.32 nm, which consisted with the (622) plane of Bi $_2$ Ti $_2$ O $_7$. Meanwhile, the SAED pattern was also point to the (622), (444), and (800) planes of Bi $_2$ Bi $_2$ O $_7$.

The X-ray diffraction patterns of different samples were shown in Fig. 2. It clearly can be seen that a new phase was introduced with the Fe doping, which should ascribe to Bi $_4$ Ti $_3$ O $_{12}$ as shown in Fig. 2a. And with the doped Fe increased, the diffraction peaks of Bi $_4$ Ti $_3$ O $_{12}$ phase would be enhanced. The structure change also would affect the optical properties, as shown in Fig. 2b. It shows that the absorbance edge extends from 440 to 550 nm, and the color of the powder turns from faint yellow to brownish black with the Fe content increase. This phenomenon was also found in the Fe-doped

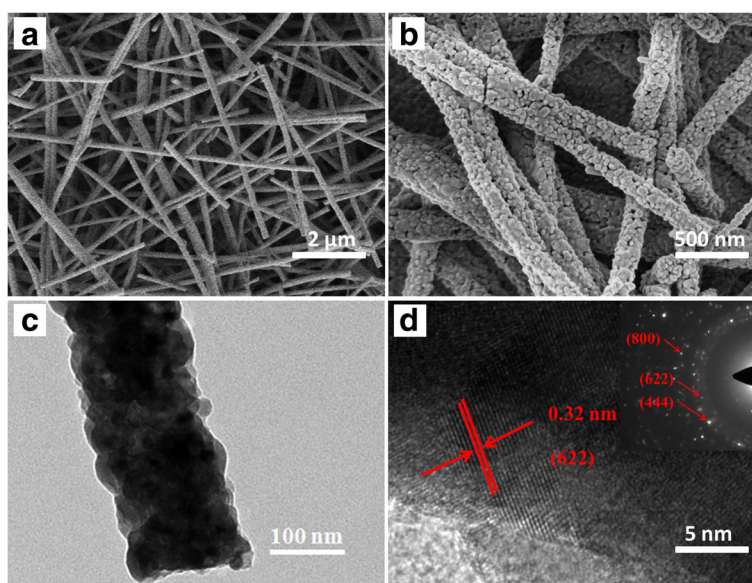


Fig. 1 SEM (a, b) and TEM (c, d) patterns of N-Fe-BTO 0.5 % samples

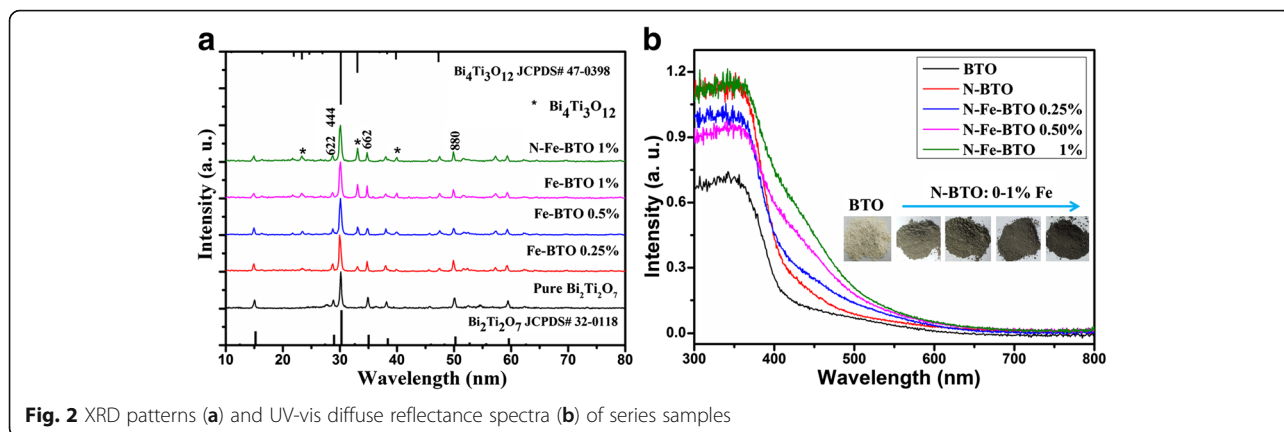


Fig. 2 XRD patterns (a) and UV-vis diffuse reflectance spectra (b) of series samples

$\text{Bi}_2\text{Ti}_2\text{O}_7$ as shown in Additional file 1: Figure S1. Obviously, this red shift should ascribe to the heterostructure between $\text{Bi}_2\text{Ti}_2\text{O}_7$ and $\text{Bi}_4\text{Ti}_3\text{O}_{12}$ phase. Additionally, it also can be seen that the absorbance edge of N-doped $\text{Bi}_2\text{Ti}_2\text{O}_7$ also shifted to longer wavelength. It means the N doping would be a key factor of the absorption properties, which can introduce an impurity energy level [14].

The photocatalytic degradation under UV light was listed in Fig. 3a, b. As can be seen, the photocatalytic activity was enhanced with increasing the Fe content. The photocatalytic activity under UV light exhibits a slight decrease if the Fe content was as high as 1%. The N-Fe-BTO 0.5% sample exhibited the best photocatalytic

activity among all the samples, which degraded 73% MO and 91% MB in 60 min while it degraded only 18% MO and 41% MB for the pure BTO sample. Additionally, it also shows that the N-BTO exhibited a much better photocatalytic activity than the pure sample, which indicated that the N doping would affect the photocatalytic activity. For the visible light, almost the same tendency was observed; the highest sample would degrade 66% MO and 87% MB in 120 min while there were only 12% MO and 36% MB for the pure BTO sample. And the N doping also would greatly enhance the photocatalytic activity, as shown in Fig. 3c, d. Obviously, the N doping also plays an important role in the

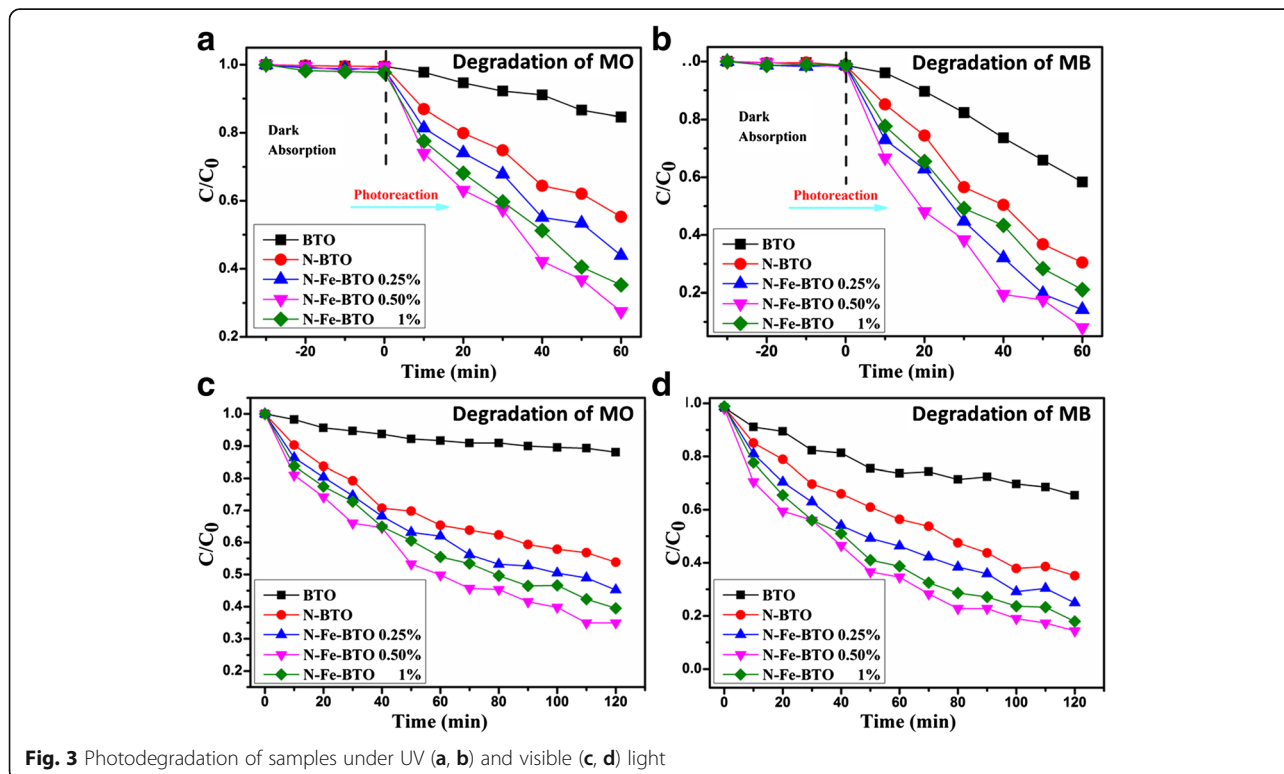
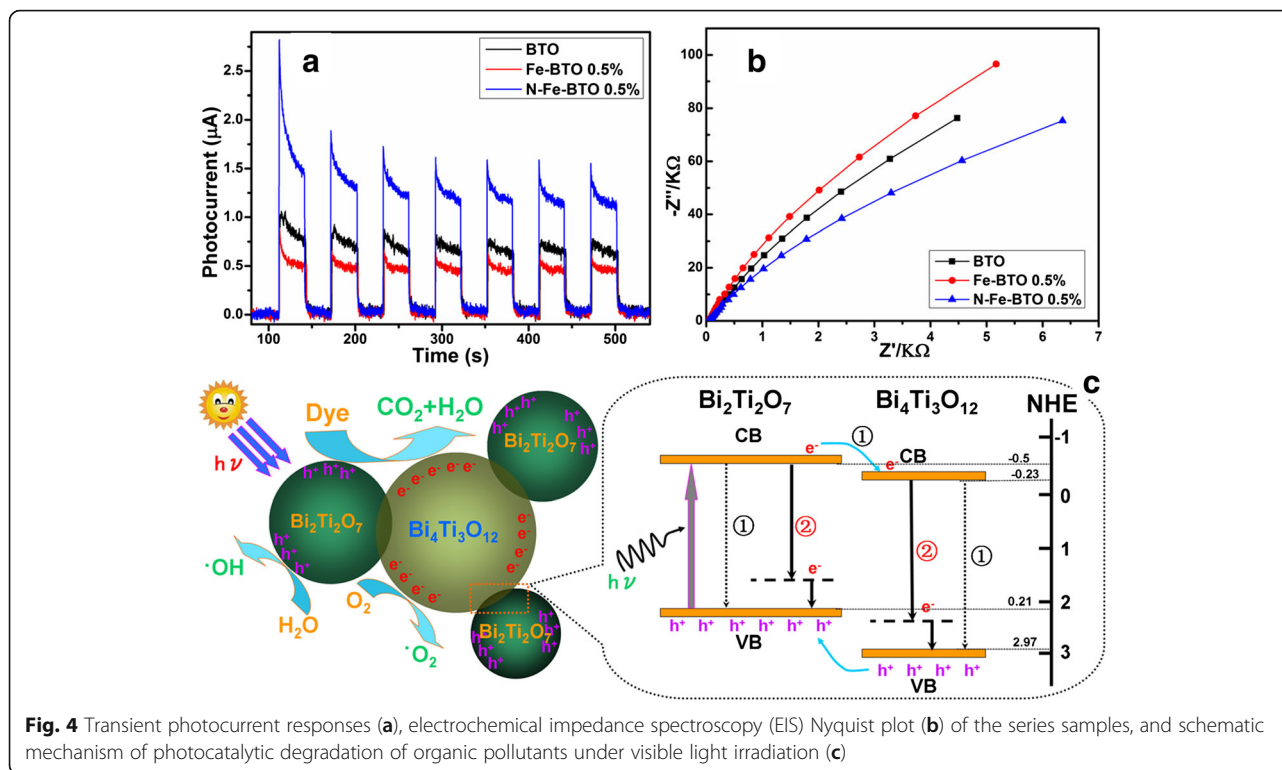


Fig. 3 Photodegradation of samples under UV (a, b) and visible (c, d) light



photocatalytic process. Overall, all the samples would prefer to degrade MB much more than MO, which should be due to its different molecular structure with different surface electric properties as shown in Additional file 1: Figure S2 [8].

For a deep investigation, the PEC system was accompanied to investigate the photophysical behaviors under visible light irradiation as shown in Fig. 4a. It was found that the photocurrent response of the Fe-BTO was slightly lower than that of the pure BTO sample, which should be due to the newly introduced $\text{Bi}_4\text{Ti}_3\text{O}_{12}$. Though this newly formed heterostructure can separate the electron-hole pairs, it also would remain the photo-generated electrons with a long time due to its huge band gap of 3.2 eV [15]. And for the N doping, it shows that the photocurrent response of N-Fe-BTO was greatly increased. According to the previous work [14], N 2p Orbital electron would affect the valence band and narrow the band gap of TiO_2 ; consequently, the N doping would narrow the band gap of BTO and accelerate the electron transfer. The EIS result also proves these results, as shown in Fig. 4b. Thus, a proposed schematic illustration can be shown in Fig. 4c. The Fe doping would result in a new phase of $\text{Bi}_4\text{Ti}_3\text{O}_{12}$. This new phase would form a heterostructure and accelerate the electron-hole pair separation as process ① showed. The photogenerated electrons from conduction band of $\text{Bi}_2\text{Ti}_2\text{O}_7$ to $\text{Bi}_4\text{Ti}_3\text{O}_{12}$ would become faster. And with the N doping, the band gap would become narrow;

subsequently, the photogenerated electrons would become more efficiently as process ② showed. And then, an enhanced photocatalytic activity can be achieved.

Conclusions

In summary, N-Fe- $\text{Bi}_2\text{Ti}_2\text{O}_7$ nanofibers were successfully synthesized by a simple method. It was found that Fe and N doping would play different roles in the photocatalytic process. A newly formed heterostructure between $\text{Bi}_2\text{Ti}_2\text{O}_7$ and $\text{Bi}_4\text{Ti}_3\text{O}_{12}$ and narrow band gap can be achieved. All of this would accelerate the charge transfer and therefore improves its photocatalytic activities.

Additional File

Additional file 1: Figure S1. UV-vis diffuse reflectance spectra of series samples. **Figure S2.** The molecular structures of the three different dyes. (DOCX 451 kb)

Acknowledgements

This work was supported by the Yongchuan Natural Science Foundation (Ycstc, 2014nc3001), Foundation of Chongqing University of Arts and Sciences (Z2013CJ01 and R2013CJ05), and Chongqing Natural Science Foundation (cstc2016shmszx20002 and cstc2016zdcy50001).

Authors' contributions

BT designed the experiment and wrote the paper. QM completed the synthesis of samples. LP and ZJ carried out the series characterization of the nanocomposites. YJ did the analysis of the data. QW gives some revision for the grammar of the manuscript. All authors read and approved the final manuscript.

Competing Interests

The authors declare that they have no competing interests.

Author details

¹Research Institute for New Materials Technology, Chongqing University of Arts and Sciences, Yongchuan, Chongqing 402160, China. ²Material and Energy Department, Southwest University, Beibei, Chongqing 400700, China. ³College of Art and Design, Chongqing University of Arts and Sciences, Yongchuan, Chongqing 402160, China. ⁴Chemical Engineering, University of Missouri, Columbia, MO 65211-2200, USA.

Received: 11 July 2016 Accepted: 2 September 2016

Published online: 08 September 2016

References

1. Fujishima A, Zhang X, Tryk DA (2008) TiO₂ photocatalysis and related surface phenomena. *Surf Sci Rep* 63:515–582
2. Maeda K (2011) Photocatalytic water splitting using semiconductor particles: history and recent developments. *J Photoch Photobio C* 12:237–268
3. Xiang Q, Yu JG, Jaroniec M (2011) Enhanced photocatalytic H₂-production activity of graphene-modified titania nanosheets. *Nanoscale* 3:3670–3678
4. Chen X, Mao SS (2007) Titanium dioxide nanomaterials: synthesis, properties, modifications, and applications. *Chem Rev* 107:2891–2959
5. Li X, Li F (2001) Study of Au/Au³⁺-TiO₂ photocatalysts toward visible photooxidation for water and wastewater treatment. *Environ Sci Technol* 35:2381–2387
6. Chen C, Ma W, Zhao J (2010) Semiconductor-mediated photodegradation of pollutants under visible-light irradiation. *Chem Soc Rev* 39:4206–4219
7. Hoffmann MR, Martin ST, Choi W, Bahnemann DW (1995) Environmental applications of semiconductor photocatalysis. *Chem Rev* 95:69–96
8. Liu BT, Peng LL (2013) Facile formation of mixed phase porous TiO₂ nanotubes and enhanced visible-light photocatalytic activity. *J Alloy Compd* 571:145–152
9. Bruton TM (1974) Study of the liquidus in the system Bi₂O₃/TiO₂. *J Solid State Chem* 9:173–175
10. Masuda Y, Masumoto H, Baba A, Goto T, Hirai T (1992) Crystal growth, dielectric and polarization reversal properties of Bi₄Ti₃O₁₂ single crystal. *Jpn J Appl Phys* 31:3108–3113
11. Knop O, Brisse F, Thermoanalytic PV (1969) X-ray, neutron, infrared, and dielectric studies of A₂Ti₂O, titanates. *Can J Chem* 47:971
12. Sankaran M, Muhammad N, Yan FY, Mowafak M, Jassim A, Vaidyanathan SJ (2010) Band-engineered bismuth titanate pyrochlores for visible light photocatalysis. *Phys Chem C* 114:10598–10605
13. Chen Y, Lu QJ, Yan XL, Mo QH, Chen Y, Liu BT, Teng LM, Xiao W, Ge LS, Wang QY (2016) Enhanced photocatalytic activity of the carbon quantum dot-modified BiOI microsphere. *Nanoscale Res Lett* 11:60
14. Gu DE, Yang BC, Hu YD (2008) V and N co-doped nanocrystal anatase TiO₂ photocatalysts with enhanced photocatalytic activity under visible light irradiation. *Cata Commun* 9:1472–1476
15. Zhao W, Jin Y, Gao CH, Gu W, Jin ZM, Lei YL, Liao LS (2014) A simple method for fabricating p–n junction photocatalyst CuFe₂O₄/Bi₄Ti₃O₁₂ and its photocatalytic activity. *Mater Chem Phys* 143:952–962

Submit your manuscript to a SpringerOpen[®] journal and benefit from:

- Convenient online submission
- Rigorous peer review
- Immediate publication on acceptance
- Open access: articles freely available online
- High visibility within the field
- Retaining the copyright to your article

Submit your next manuscript at ► springeropen.com
